Broadband continuous-variable entanglement source using a chirped poling nonlinear crystal

J. S. Zhao, L. Sun, X. Q. Yu, J. F. Wang, H. Y. Leng, Z. D. Xie, Y. L. Yin, P. Xu,* and S. N. Zhu†
National Laboratory of Solid State Microstructures and Department of Physics, Nanjing University, Nanjing 210093, People's Republic of China
(Received 3 July 2009; published 28 January 2010)

Aperiodically poled nonlinear crystal can be used as a broadband continuous-variable entanglement source and has strong stability under perturbations. We study the conversion dynamics of the sum-frequency generation and the quantum correlation of the two pump fields in a chirped-structure nonlinear crystal using the quantum stochastic method. The results show that there exists a frequency window for the pumps where two optical fields can perform efficient upconversion. The two pump fields are demonstrated to be entangled in the window and the chirped-structure crystal can be used as a continuous-variable entanglement source with a broad response bandwidth.

DOI: 10.1103/PhysRevA.81.013832 PACS number(s): 42.65.Ky, 42.65.Lm, 03.67.Bg

I. INTRODUCTION

Quantum entanglement plays an indispensable role in quantum information and quantum communication [1] nowadays. Therefore, the preparation of quantum entanglement states is a basic work of quantum information science. Continuous-variable (CV) entanglement has attracted much attention due to its efficiency in quantum information and application in universal quantum computation [2]. CV entanglement was also used to demonstrate the Einstein-Podolsky-Rosen (EPR) paradox [3–6]. Recently, the quasiphase-matching (QPM) technique was introduced into the entanglement source and attracted great attention due to its high conversion efficiency and also its flexibility on modulating phase-matching wavelength [7–11]. In the QPM device, nonlinear optical processes can be controlled by the proper design of the modulation structure of nonlinearity. For example, chirped structure can be used to broaden the bandwidth of sum-frequency generation (SFG) [12] and generate broadband entangled photons through the spontaneous parametric down conversion (SPDC) process [13,14].

In this work we propose a scheme to generate broadband CV entanglement from the chirped poling nonlinear crystal. We will discuss the sum-frequency dynamics and then analyze the correlation property of two pump fields with lower frequencies using the quantum stochastic method [15]. The results show that there exists a response window where the pump fields with frequencies in a certain range can perform efficient upconversion. Within this window, the two fields of lower frequency are entangled. Therefore, the chirped-structure nonlinear crystal can be used as a broadband CV entanglement generator. A CV entanglement source with a broad response bandwidth has practical advantages. It can not only improve adaptability and flexibility of the source in practical use, but also improve the stability of the source under external turbulences. External perturbations such as temperature instability can result in phase mismatch and may greatly reduce the conversion efficiency. The chirped crystal can overcome this problem due to its large response bandwidth.

*pingxu520@nju.edu.cn
†zhusn@nju.edu.cn

II. THEORETICAL MODEL AND METHOD

Sum-frequency generation couples three electromagnetic fields in a nonlinear crystal with the second-order susceptibility $\chi^{(2)}$. For the chirped poling crystal shown in Fig. 1, the ferroelectric domains of the crystal are regularly reversed to provide a chirped spatial frequency represented by $2\pi/\Lambda(z)$, where $\Lambda(z)$ is the reversion period. We can take the spatial frequency form of the crystal as $K_0 - \alpha z$, where K_0 is the initial spatial frequency determined by the structure at the left end of the crystal and α is the chirp degree that represents the degree of the linear chirp. The functional form of the spatially varying nonlinearity is $\exp(i\int_0^z \alpha z dz) = \exp(i\alpha z^2/2)$ [13].

To examine the interaction property along the crystal, we study the sum-frequency generation process in the traveling-wave regime. Two pump beams with frequencies ω_1 and ω_2 enter the chirped-structure crystal from the left end at $z = 0$ and three optical fields with frequencies ω_1, ω_2, and ω_3 ($\omega_3 = \omega_1 + \omega_2$) exit the crystal at $z = L$. We follow the approach of Huntter *et al.*, [16] by quantizing the three interacting fields in terms of the photon fluxes rather than the energy densities. As we know, in quantum field theory, the generator for time evolution is the Hamiltonian operator and the generator for space propagation is the momentum operator. We can write the nonlinear momentum operator, after including the effect of chirped structure, as follows

$$G_{nl}(z) = i\hbar\kappa[\hat{b}(\omega_1, z)\hat{b}(\omega_2, z)\hat{b}^\dagger(\omega_3, z)Q(\Delta k, z) - \hat{b}^\dagger(\omega_1, z)\hat{b}^\dagger(\omega_2, z)\hat{b}(\omega_3, z)Q^*(\Delta k, z)]. \quad (1)$$

Here $\hat{b}^\dagger(\omega_m, z)$ and $\hat{b}(\omega_m, z)$ are the creation and annihilation operators creating or annihilating one photon of frequency ω_m at point z during the chosen time interval. κ is the effective conversion coefficient. The bosonic operators $\hat{b}^\dagger(\omega_m, z)$ and $\hat{b}(\omega_m, z)$ obey the spatial commutation relation $[\hat{b}(z, \omega_m), \hat{b}^\dagger(z', \omega_n)] = \delta_{m,n}\delta(z' - z)$. Q is associated with the initial wave-vector mismatch of the three coupled fields and also the chirp degree. It has the form $Q = e^{i\Delta k\cdot z}e^{-i\alpha z^2/2}$, where $\Delta k = k_1 + k_2 + K_0 - k_3$ is the initial wave-vector mismatch.

The equation of motion for the density matrix of the system is governed by [17]

$$i\hbar\frac{\partial\rho(z)}{\partial z} = [\rho(z), G_{nl}(z)]. \quad (2)$$

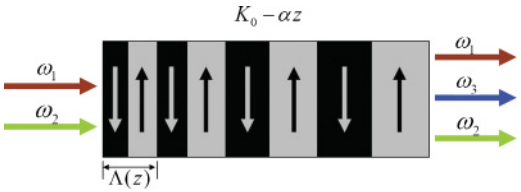

FIG. 1. (Color online) Sum-frequency generation in chirped poling nonlinear crystal. ω_1 and ω_2 denote the frequencies of the two pump fields and $\omega_3 = \omega_1 + \omega_2$ denotes the sum-frequency field. The poling period $\Lambda(z)$ is chosen so that the corresponding spatial frequency $2\pi/\Lambda(z)$ is linearly chirped.

This equation provides a full description of the three interacting fields. Theoretically, the density matrix $\rho(z)$ implies all the statistical properties of the system. However, it is very difficult to find the analytical solution for this equation. Therefore, we use the stochastic method to examine the correlation property of the system. Following the usual procedure [18], we transform the equation of motion of the density matrix to a Fokker-Plank equation in the P representation [19,20]. After the transformation, the Fokker-Plank equation reads

$$\begin{aligned}\frac{dP}{dz} = \Bigg\{\kappa\Bigg[&-\frac{\partial}{\partial\beta_1}\beta_2^*\beta_3 Q^* - \frac{\partial}{\partial\beta_2}\beta_1^*\beta_3 Q^* - \frac{\partial}{\partial\beta_1^*}\beta_2\beta_3^* Q \\ &- \frac{\partial}{\partial\beta_2^*}\beta_1\beta_3^* Q + \frac{\partial}{\partial\beta_3}\beta_1\beta_2 Q + \frac{\partial}{\partial\beta_3^*}\beta_1^*\beta_2^* Q^*\Bigg] \\ &+ \frac{1}{2}\kappa\Bigg[\left(\frac{\partial^2}{\partial\beta_1\partial\beta_2} + \frac{\partial^2}{\partial\beta_2\partial\beta_1}\right)\beta_3 Q^* \\ &+ \left(\frac{\partial^2}{\partial\beta_1^*\partial\beta_2^*} + \frac{\partial^2}{\partial\beta_2^*\partial\beta_1^*}\right)\beta_3^* Q\Bigg]\Bigg\} P(\vec{\beta}_i, \vec{\beta}_i^*, z). \end{aligned} \quad (3)$$

According to the stochastic differential equation theory [21,22], the Fokker-Plank equation is equivalent to a set of stochastic equations in the positive-P representation. These equations are listed as follows

$$\begin{aligned}\frac{d\beta_1}{dz} &= \kappa\beta_2^+\beta_3 Q^* + \sqrt{\kappa\beta_3 Q^*/2}(\eta_1 + i\eta_2), \\ \frac{d\beta_2}{dz} &= \kappa\beta_1^+\beta_3 Q^* + \sqrt{\kappa\beta_3 Q^*/2}(\eta_1 - i\eta_2), \\ \frac{d\beta_1^+}{dz} &= \kappa\beta_2\beta_3^+ Q + \sqrt{\kappa\beta_3^+ Q/2}(\eta_3 + i\eta_4), \\ \frac{d\beta_2^+}{dz} &= \kappa\beta_1\beta_3^+ Q + \sqrt{\kappa\beta_3^+ Q/2}(\eta_3 - i\eta_4), \\ \frac{d\beta_3}{dz} &= -\kappa\beta_1\beta_2 Q, \\ \frac{d\beta_3^+}{dz} &= -\kappa\beta_1^+\beta_2^+ Q^*. \end{aligned} \quad (4)$$

In these equations, $\eta_i (i = 1, 2, 3, \text{and } 4)$ are real Gaussian noise terms that satisfy the correlation condition $\langle\eta_i(z)\eta_j(z')\rangle = \delta_{ij}\delta(z - z')$. β and β^+ are treated as independent complex variables due to the independence of the real noise terms [23]. β^+ and β^* are equal only in the statistical sense.

We will investigate the frequency conversion dynamics and the quantum properties of the system. The stochastic positive-P representation is very convenient for calculating any normally ordered operator moments. The expectation value of the operator can be obtained by taking an average over the product of c-numbers from a large number of trajectories

$$\langle(b^\dagger)^m b^n\rangle \rightarrow \overline{((\beta^+)^m\beta^n)}. \quad (5)$$

This relationship holds where there are no divergence problems in the integration, as is satisfied in the system we present here. In this case, the average photon number, which is proportional to the intensity of the optical field, is of great interest and can be calculated through the averaging process $\overline{(\beta^+\beta)}$.

To examine the entanglement property between the two pump fields output from the crystal, we will use the entanglement criteria developed by Duan *et al.*, [24] based on the inseparability of the density matrix. First, we introduce two quadrature operators $X_i = \hat{b}_i + \hat{b}_i^\dagger$ and $Y_i = -i(\hat{b}_i - \hat{b}_i^\dagger)$, which are similar to the dimensionless position and momentum operators in the harmonic oscillator. For the two-mode case, we can define two combined quadratures [25] $X_+ = X_1 + X_2$ and $Y_- = Y_1 - Y_2$. According to the entanglement criteria, if the variances of the two combined quadratures satisfy the inequality

$$[V(X_+) + V(Y_-)]/4 < 1, \quad (6)$$

these two modes should be regarded as entangled modes. The variance presented here can be obtained using $V(X) = \overline{X^2} - (\overline{X})^2$ in the positive-P representation.

III. NUMERICAL CALCULATION AND DISCUSSION

The sum-frequency dynamics were discussed in the phase-matching scheme previously from both quantum [25] and classical [26] approaches. The chirped structure mainly introduces spatially modulated wave-vector mismatch among the coupled waves. It is obvious that if the chirp degree $\alpha = 0$, Δk should also be zero to satisfy the phase-matching condition. In this case, the chirped crystal will change into a periodically poled QPM (PPQPM) crystal and the SFG can be regarded as QPM. In the following part, we first investigate the SFG dynamics and the CV entanglement in PPQPM crystal. The results can be compared with the chirped poling crystal. The intensities of the two pump fields and the SFG fields are shown in Fig. 2(a). As seen from the figure, they vary along the propagation direction in the crystal. The curve is calculated by integrating the stochastic Eq. (4) numerically and taking an average over 3×10^6 trajectories for $\kappa = 0.01$ with the initial conditions $\beta_1(0) = \beta_2(0) = \beta(0) = 1000/\sqrt{2}$ and $\beta_3(0) = 0$.

We can see that the two input beams with equal photon numbers are converted into a higher frequency field. With the increase of the interaction length, the conversion efficiency may attain almost 100% theoretically. The correlation of the two pump fields in the QPM condition is shown in Fig. 2(b), which emerges from the sum-frequency generation. With the increase of the conversion ratio, the correlation value decreases from 1 to 0 until the backflow process occurs. Thus it indicates that the higher the upconversion efficiency is, the stronger the entanglement of the two pump fields can be obtained. The results are consistent with former conclusions [25]. It should be noted that the strongest entanglement requires unit conversion efficiency. In this case, though the vacuum noises are perfectly correlated, the average intensities of the pumps will become

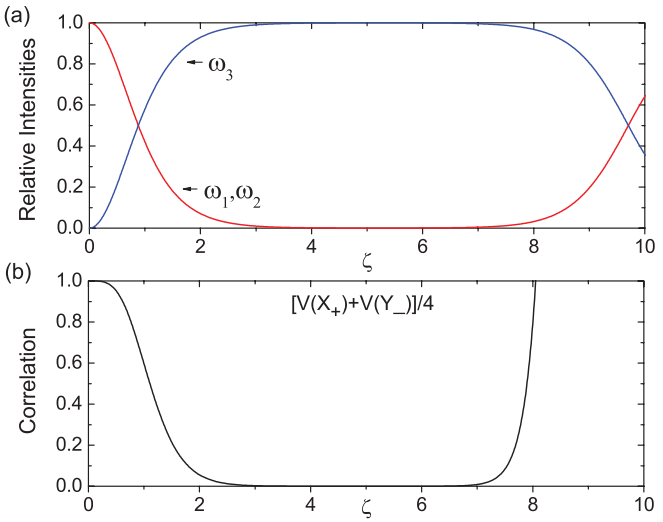

FIG. 2. (Color online) (a) Mean relative intensities in periodically poled QPM crystal. The intensities are calculated by taking an average over 3×10^6 stochastic trajectories of the positive-P equation (4). The horizontal axis is the scaled dimensionless length $\zeta = \kappa\,|\beta(0)|\,z$ and the vertical axis are the relative intensities with respect to $N(0) = |\beta(0)|^2$. The parameters are chosen as $\kappa = 0.01$, $\beta_1(0) = \beta_2(0) = \beta(0) = 1000/\sqrt{2}$, and $\beta_3(0) = 0$. (b) The correlation value according to Duan *et al.*, [24] in periodically poled QPM crystal. Note that the quantities in this and the subsequent graphs are all dimensionless.

zero. Therefore, it cannot be used as a bright source at this point.

We now turn to the general case where α is a nonzero constant. For convenience of calculation, we use the scaled dimensionless chirp degree parameter $A = \alpha/(\kappa\,|\beta(0)|)^2$ and initial wave-vector mismatch $\Delta S = \Delta k/\kappa\,|\beta(0)|$. A typical result for the evolution of field intensities in the crystal is shown in Fig. 3 with $A = 8$ and $\Delta S = 10/\sqrt{2}$. We can see that the two pump-field intensities appear to stay unchanged until they enter a strong interaction area called the effective interaction length L_{eff}. After the strong interaction, the three fields keep almost stable intensities, respectively, except that each exhibits small oscillations. This is not difficult to understand from the phase-matching condition in the chirped structure: The phase is only approximately matched within L_{eff}, thus before or after this area the phase mismatch inhibits efficient sum-frequency generation.

The effective interaction length L_{eff} will become shorter while the chirp degree α increases [12]. This will also lead to lower conversion efficiency under the same initial conditions. The initial wave-vector mismatch Δk at the left end of the crystal affects the position of L_{eff} in the crystal. With Δk increasing, the position of L_{eff} will move toward the right end of the crystal until it exits the output surface.

We now continue to investigate the correlation property of the two pump fields. As shown in Fig. 4, the correlation value stays around 1 initially and then quickly decreases to the minimum, followed by a wave-like pigtail with its average value slowly increasing. This is in coincidence with the upconversion process: The strong interaction of the three fields within the effective length leads to a quick decrease of the correlation value; after the strong interaction, the correlation

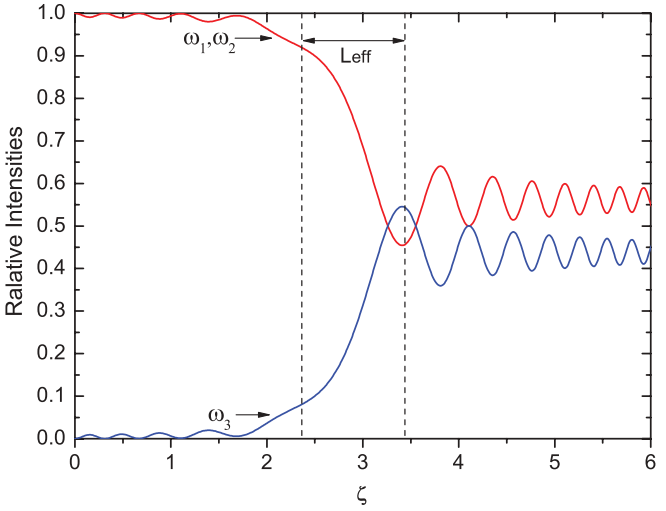

FIG. 3. (Color online) Mean relative intensities in chirped-structure crystal. The intensities are calculated by taking an average over 3×10^6 stochastic trajectories with $A = 8$ and $\Delta S = 10/\sqrt{2}$, where $A = \alpha/(\kappa\,|\beta(0)|)^2$ and $\Delta S = \Delta K/\kappa\,|\beta(0)|$ are the scaled dimensionless chirp factor and the initial spatial frequency mismatch. L_{eff} is the effective interaction length in the crystal. Other parameters are the same as those in Fig. 1.

value stays below 1 for some distance. The small oscillations of the correlation value result from the small upconversion and inverse processes after the strong interaction. The slow increase of the average correlation value may be a consequence of the stochastic process. Figure 4 demonstrates that it is the effective nonlinear process that guarantees the strong correlation. Here the two pump fields become entangled with each other and are converted to a field of higher frequency. The higher the conversion efficiency is the stronger the correlation becomes. In Fig. 4 the conversion efficiency is only around 50%, so these two pump fields are not perfectly correlated. This is in agreement with what is discussed in the PPQPM situation where perfect correlation requires unit conversion efficiency.

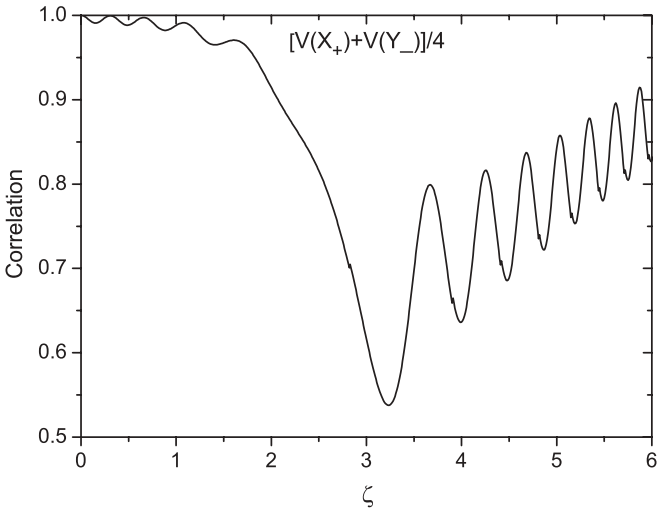

FIG. 4. The correlation according to Duan *et al.*, [24] in the chirped structure crystal. The parameters are the same as those in Fig. 3.

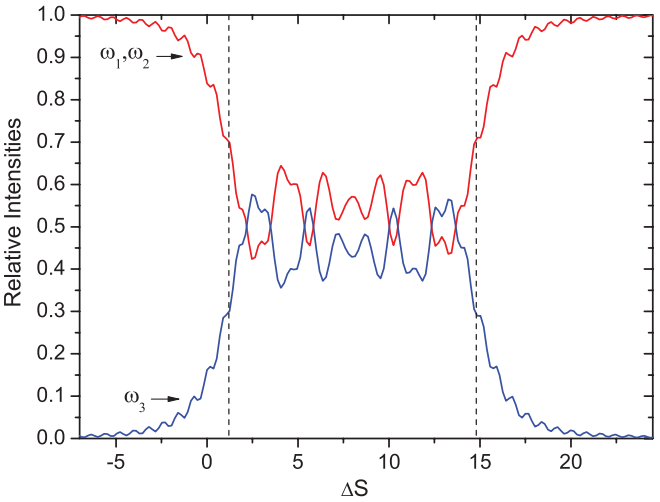

FIG. 5. (Color online) Upconversion efficiency as a function of the initial wave-vector mismatch. The horizontal axis is the scaled dimensionless wave-vector mismatch. The parameters are chosen as $\kappa = 0.01, \beta_1(0) = \beta_2(0) = \beta(0) = 1000/\sqrt{2}, \beta_3(0) = 0$, and $A = 8$. The output surface is at $\zeta = 4$.

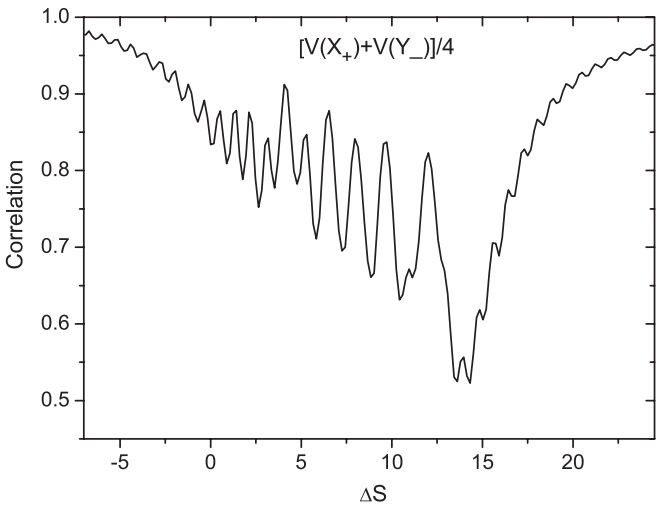

FIG. 6. The Duan [24] correlation as a function of the initial wave-vector mismatch. The parameters are the same as those in Fig. 5.

According to the conversion property, we can predict a broad response bandwidth of the crystal since the effective interaction length is small compared to the entire nonlinear crystal. The spatial frequencies located at $z = 0$ and $z = L$ will set the minimum and maximum of the input frequency. In a practical chirped poling crystal, K_0 is fixed and the initial wave-vector mismatch Δk reflects the input frequencies due to the dispersion relation of the crystal, that is, $k = \omega_i n(\omega_i)/c$, where $n(\omega_i)$ is the refractive index of the field with frequency ω_i. To demonstrate the frequency response property of the chirped-structure crystal, we set the crystal length $\zeta = 4$ and describe the relative intensities of the three fields at the output surface of the crystal as a function of initial wave-vector mismatch. As shown in Fig. 5, there exists a window for the initial wave-vector mismatch, where the upconversion efficiency stays around 50% except for some fluctuations. The correlation property of the two pump fields in the response window is shown in Fig. 6. It is clear that the two pump fields are entangled within the window. The fluctuations can be ascribed to the small oscillation of the upconversion efficiency. Since the conversion efficiency within the window cannot reach 100%, these two pump fields are not perfectly correlated. Nevertheless, these two entangled fields are of considerable intensity and thus can be used as bright sources.

We can understand the window by reexamining the reciprocal vector property of the chirped structure. As we know, in periodically poled crystals where poling periods are designed to meet particular phase-matching conditions, the periodical structure can only provide one or some discrete reciprocal vectors, thus only those fields with designated frequencies can perform efficient upconversion and the bandwidth is set by the phase-matching bandwidth. In contrast, the chirped structure contains a variable period of domain modulation, thus it can provide various reciprocal vectors. It has much more reciprocal vectors than the periodically poled crystal. Different reciprocal vectors work for different sum-frequency processes. It is the increase in the number of reciprocal vectors that makes possible the upconversion of a wide range of frequencies. Therefore, the chirped crystal can respond to a wide range of frequencies with considerable efficiency. In other words, if the input fields contain a bandwidth equivalent to this frequency window, the upconversion will take place with almost the same efficiency within the window. In this sense, the CV entanglement is broadband.

The conversion window also provides another advantage of the chirped structure. It can improve the stability of the entanglement source under external perturbations such as temperature fluctuation and mechanical vibration. For example, temperature fluctuations can affect the refractive index of the crystal, which introduces wave-vector mismatch. This is equivalent to the frequency change of input fields. The mechanical vibration may also lead to the divergence of the incident angle, which may then result in phase mismatch. Fortunately, the chirped crystal contains a broad response window for the input fields and therefore can compensate for the mismatch. In this sense, the chirped structure also renders the entanglement source more robust and stable.

IV. CONCLUSION

We use the stochastic method to study the dynamics of the nonlinear sum-frequency process in a chirped QPM crystal. The correlation property of the two pump fields are investigated in detail. Our results show that there exists a wide frequency response window in the chirped structure where the pump fields can perform an efficient upconversion. The pump fields are well entangled in the window due to nonlinear interaction. In other words, the chirped-poled QPM crystal can be used as a CV entanglement source with a broad response bandwidth. The chirped structure can also be used to improve the stability under external disturbances.

ACKNOWLEDGMENTS

This research was supported by the National Natural Science Foundations of China under Contract No. 60578034 and the State Key Program for Basic Research of China (No. 2006CB921804).

[1] M. A. Nielsen and I. L. Chuang, *Quantum Computation and Quantum Information* (Cambridge University Press, Cambridge, United Kingdom, 2000).
[2] S. L. Braunstein and P. V. Loock, Rev. Mod. Phys. **77**, 513 (2005).
[3] M. D. Reid, Phys. Rev. A **40**, 913 (1989).
[4] M. K. Olsen, Phys. Rev. A **70**, 035801 (2004).
[5] A. I. Lvovsky and M. G. Raymer, Rev. Mod. Phys. **81**, 299 (2009).
[6] S. Pirandola, S. Mancini, S. Lloyd, and S. L. Braunstein, Nature Physics **4**, 726 (2008).
[7] J. A. Armstrong, N. Bloembergen, J. Ducuing, and P. S. Pershan, Phys. Rev. **127**, 1918 (1962).
[8] P. A. Franken and J. F. Ward, Rev. Mod. Phys. **35**, 23 (1963).
[9] S. Matsumoto, E. J. Lim, H. M. Hertz, and M. M. Fejer, Electoron. Lett. **27**, 2040 (1991).
[10] M. A. Arbrore, A. Galvanauskas, D. Harter, M. H. Chou, and M. M. Fejer, Opt. Lett. **22**, 1341 (1997).
[11] S. N. Zhu, Y. Y. Zhu, and N. B. Ming, Science **278**, 843 (1997).
[12] H. Suchowski, D. Oron, A. Arie, and Y. Silberberg, Phys. Rev. A **78**, 063821 (2008).
[13] S. E. Harris, Phys. Rev. Lett. **98**, 063602 (2007).
[14] M. B. Nasr, S. Carrasco, B. E. A. Saleh, A. V. Sergienko, M. C. Teich, J. P. Torres, L. Torner, D. S. Hum, and M. M. Fejer, Phys. Rev. Lett. **100**, 183601 (2008).
[15] D. F. Walls and G. J. Milburn, *Quantum Optics* (Springer-Verlag, Berlin, 1994).
[16] B. Huttner, S. Serulnik, and Y. Ben-Aryeh, Phys. Rev. A **42**, 5594 (1990).
[17] Y. R. Shen, Phys. Rev. **155**, 921 (1967).
[18] C. W. Gardiner, *Quantum Noise* (Springer, Berlin, 1991).
[19] R. J. Glauber, Phys. Rev. **131**, 2766 (1963).
[20] E. C. G. Sudarshan, Phys. Rev. Lett. **10**, 277 (1963).
[21] P. D. Drummond and C. W. Gardiner, J. Phys. A **13**, 2353 (1980).
[22] C. W. Gardiner, *Handbook of Stochastic Methods* (Springer-Verlag, Berlin, 1985).
[23] M. K. Olsen, L. I. Plimak, M. J. Collett, and D. F. Walls, Phys. Rev. A **62**, 023802 (2000).
[24] L. M. Duan, G. Giedke, J. I. Cirac, and P. Zoller, Phys. Rev. Lett. **84**, 2722 (2000).
[25] M. K. Olsen and A. S. Bradley, Phys. Rev. A **77**, 023813 (2008).
[26] R. W. Boyd, *Nonlinear Optics* (Academic Press, Amsterdam, 2003).